Vertical Beam Size Measurement of the SPring-8 Storage Ring by Visible Synchrotron Radiation Interferometer

Mitsuhiro MASAKI, Shiro TAKANO, Hitoshi TANAKA, Kouichi SOUTOME, Masaru TAKAO, Masaya OISHI, Kazuhiro TAMURA, Masazumi SHOJI, Shigeki SASAKI and Haruo OHKUMA

SPring-8
Mikazuki, Sayo-gun, Hyogo 679-5198, Japan

Abstract

The vertical beam size of the SPring-8 storage ring was measured by a visible synchrotron radiation interferometer. The measurements were performed at various working points of the storage ring. It was observed that the vertical beam size increased with an increase in the coupling ratio of emittance. The vertical beam size was less than 20μm (rms) at the ordinary usertime operation where the coupling ratio was below 0.1%. The filling dependence of the vertical beam size was measured at a beam current of 99mA with small coupling ratio below 0.1%. The vertical beam size steeply increased with a filling factor above 47/48.

1. Introduction

In the case of the SPring-8 storage ring, it is deduced that the emittance is about 6.8nmrad and the coupling ratio of emittance is less than 0.1% on the usertime operation [1]. It is expected that the vertical beam size is less than 20μm (rms) at the source point of the visible light diagnostic beamline, where the vertical betatron function is 26m.

Imaging of the visible synchrotron radiation (SR) is one of conventional methods of beam size measurement. The resolution of imaging is generally limited by diffraction phenomena. The diffraction limited resolution is no better than 50μm (rms) at the visible wavelength in the case of the SPring-8 storage ring [2]. It is difficult to measure the vertical beam size of the storage ring by imaging the visible SR.

A SR interferometer is one of the suitable devices for measurements of small beam size and first applied by Mitsuhashi et al[3]. In order to measure the vertical beam size, a SR interferometer was installed in the visible light diagnostic beamline of the SPring-8 storage ring. The experimental setup and the results of measurements are described in this report.

2. Experimental Setup

A SR interferometer was installed in the visible light diagnostic beamline of which the source point is in the B2 bending magnet of the cell 38. The experimental setup is shown in Fig.1. The interferogram formed by a diffracting mask with double slit was imaged on a CCD camera by two achromatic doublet lenses. The angular separation of two slits on the double slit is 2.25mrad from view of the light source point and the width of each slit is 1mm. We used two mirrors to steer visible SR to the interferometer. The reflection planes of the mirrors are aluminum coating protected by membrane MgF_2 on the polished glass base. The flatness of the mirrors are better than $\lambda/10$ ($\lambda = 632.8$nm). The heat load to the mirror in vacuum is absorbed by a water-cooled x-ray absorber. The mirror in vacuum is not water-cooled to reduce the vibration. The view window is made of a sapphire glass 4mm thick, of which the flatness is unknown. We should choose a shorter wavelength to measure small beam size with sufficient resolution. The monochromatic light was obtained by a bandpass filter attached to the CCD camera, of which the center wavelength and the bandwidth are 441.6nm and 10nm(FWHM), respectively. A linear polarizer was placed in front of the CCD camera to select σ-polarized component. All the instruments of the SR interferometer are installed in the accelerator tunnel.

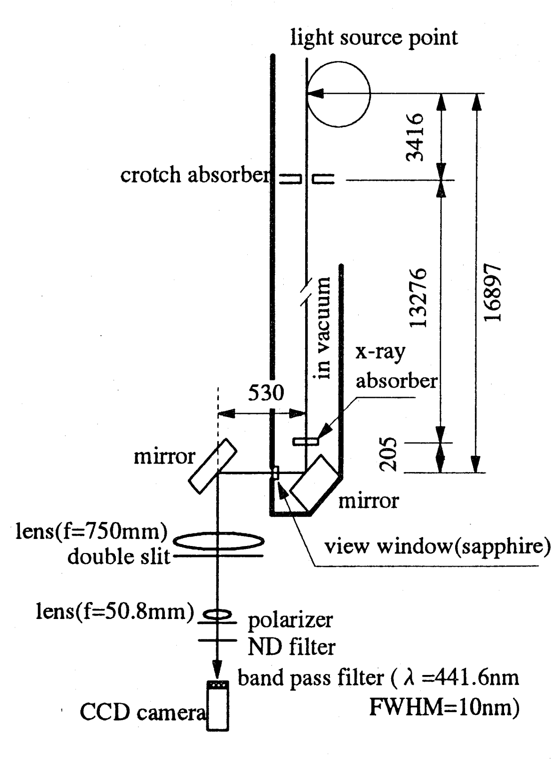

Fig. 1 Schematic view of the visible light diagnostic beam line and the SR interferometer.

3. Visibility

A typical observed interferogram is shown in Fig.2. The visibility F is defined by the maximum and minimum intensities Imax, Imin of the interferogram as follows,

$$F = \frac{I_{max} - I_{min}}{I_{max} + I_{min}} \quad . \qquad (1)$$

Since the visibility calculated by eq. (1) is sensitive to the fluctuation of the maximum and minimum intensities due to noise, the visibility is obtained by the fitting the following formula to data,

$$I = A \exp\left[-\frac{(y - y_0)^2}{2a^2}\right]\left\{1 + F\cos(ky + \phi)\right\} \quad (2)$$

where A, a, y_0, F, k, ϕ are free parameters. The Gaussian function is introduced as an approximation of the sinc function envelope formed by the finite width (1mm) of the slits. The fitting was performed after subtracting the background from the measured data.

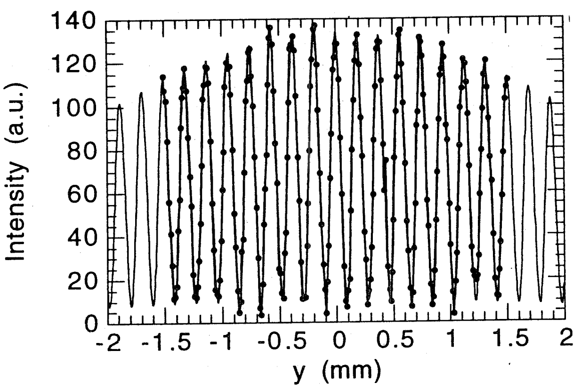

Fig. 2 A typical interferogram. The dots are measured data and the solid line is fitted curve by eq. (2).

Assuming that the equilibrium transverse distribution of the electron beam is Gaussian function and the SR has spherical wavefront, the relation between the visibility F and the beam size σ is given by the following formula,

$$F = \exp\left[-2\left(\frac{\pi\theta\sigma}{\lambda}\right)^2\right] \qquad (3)$$

where λ is wavelength of light, θ is angular separation of the double slit from view of the light source point.

4. Results and Discussions

4.1 Vertical beam size versus coupling ratio of emittance

In order to examine the sensitivity of the SR interferometer for small beam size and to estimate the vertical beam size at the usertime operation, measurements were performed by varying coupling ratio of emittance. The working points are shown on the tune diagram in Fig. 3. The condition of the beam was 21 equal spacing bunches with 1mA/bunch. The coupling ratio was derived from the following formula under the single resonance approximation,

$$\kappa = \frac{C^2}{2(\nu_I - \nu_{II})^2 - C^2} \qquad (4)$$

where C = 0.0055 is the measured minimum tune separation, ν_I and ν_{II} are the measured betatron tunes.

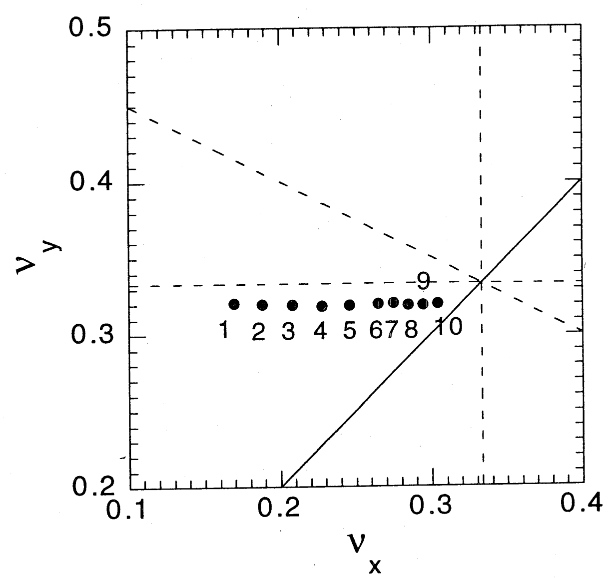

Fig. 3 The working points on the tune diagram. The vertical beam sizes were measured on the working points denoted by the numbered dots. The working point at the usertime operation is No.1. The solid and broken lines show the 2nd and 3rd order resonances, respectively.

The vertical beam sizes measured by the SR interferometer increased with an increase in the coupling ratio as shown in Fig. 4. The experimental data well agreed with the following theoretical curve above the coupling ratio 0.2%,

$$\sigma_y = \sqrt{\varepsilon\beta_y\frac{\kappa}{1+\kappa} + \left(\eta_y\frac{\Delta E}{E}\right)^2} \qquad (5)$$

where ε = 6.8nmrad is the emittance, βy = 25.94m is the vertical betatron function at the light source point, κ is the coupling ratio of emittance, ηy = 5.7mm is the spurious dispersion and $\Delta E/E$ = 1.1e-3 is the beam energy spread. The measured beam size is slightly larger than the theoretical size given by eq.(5) below the coupling ratio 0.2%. We consider that the possible instrumental reasons of discrepancies are wavefront distortion due to poor flatness of the view window and contamination of the stray light caused by reflections inside the narrow vacuum chambers.

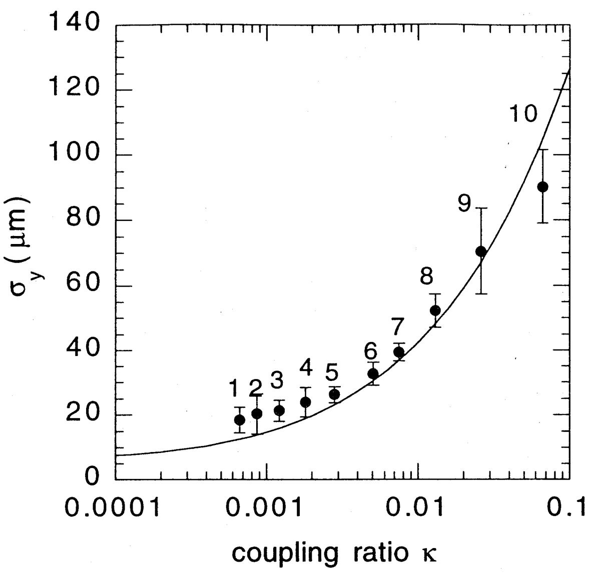

Fig. 4 Vertical beam size versus coupling ratio of emittance. The dots show the measurement results at 21 equal spacing bunches with 1mA/bunch. The numbers with data show the working points in Fig.3. The solid line is the theoretical curve given by eq.(5).

4.2 Filling dependence of vertical beam size

It was deduced from the measurement of Touscheck lifetime of the SPring-8 storage ring that the bunch volume expanded when the filling factor increased above 47/48. Since the vertical beam size is small in comparison with the horizontal and longitudinal beam sizes, it is expected that the increase of vertical beam size dominates the bunch volume expansion.

The filling dependence of the vertical beam size was measured on the working point of usertime operation at a stored beam current of 99mA. The measurements were performed with filling factors of 2/3, 47/48, 95/96 and 1 (uniform). The expansion ratio, i.e. the ratio of the vertical beam size at the each filling factor to the one at filling factor 2/3, is shown in Fig.5. We see that the vertical beam size is steeply expanded above the filling factor 47/48. The size expansion ratio of the uniform fill is 2.3 compared with the filling factor 2/3. One possible mechanism of the beam size expansion is considered as the ion-trap phenomena and the detailed investigation is in progress.

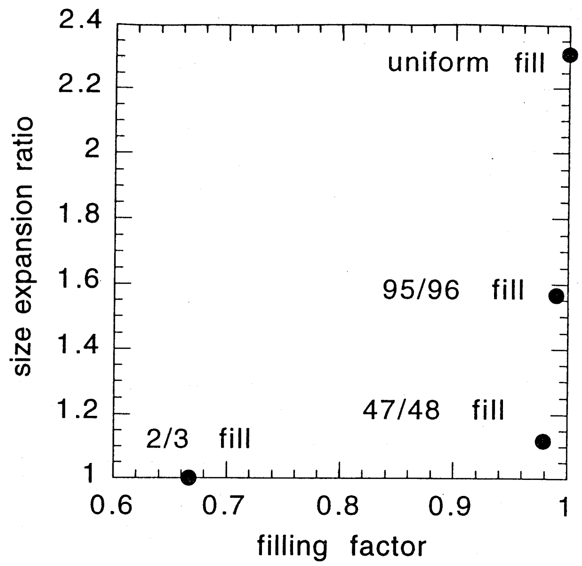

Fig. 5 The filling dependence of the vertical beam size at 99mA. The beam size steeply increased with filling factors above 47/48.

5. Conclusion

The vertical beam size of the SPring-8 storage ring was measured by a visible SR interferometer. An increase of the vertical beam size with an increase in the coupling ratio of emittance was observed by measurements at the various working points of the storage ring. The measured vertical beam size well agreed with the theoretical curve except the working points having coupling ratio smaller than 0.2%, where the data were slightly larger than theoretical size. We consider that the possible instrumental reasons of discrepancies are wavefront distortion due to poor flatness of the view window and contamination of the stray light caused by reflections inside the narrow vacuum chambers. Since these instrumental effects generally reduce the visibility, the measured small beam size of 20µm(rms) should be regarded as upper limit.

The filling dependence of the vertical beam size was measured on the working point of usertime operation at the beam current of 99mA. A steep expansion of vertical beam size was observed for the filling factors above 47/48. The expansion ratio of the uniform fill was 2.3 compared with the filling factor 2/3. One possible mechanism of this beam size expansion is considered as the ion-trap phenomena and the detailed investigation is in progress.

References

[1] M. Takao, et al., Proceedings of the 1999 Particle Accelerator Conference, N.Y.,1999, p.2349
[2] M. Masaki, et al., SPring-8 Ann. Rep. 1997, p.169
[3] T. Mitsuhashi, et al., Proceedings of the 1999 Particle Accelerator Conference, N.Y.,1999, p.492